SLAC-PUB-7227
ICHEP-96 PA05-085
July/22/96

Measurement of the B^+ and B^0 Lifetimes with Topological Vertexing at SLD *

The SLD Collaboration**

Abstract

The lifetimes of the B^+ (B_u) and B^0 (B_d) mesons have been measured using a sample of 150,000 hadronic Z^0 decays collected by the SLD experiment at the SLC between 1993 and 1995. The analysis reconstructs the decay length and charge of the B meson using a novel topological technique. This method results in a high statistics sample of 6033 (3665) charged (neutral) vertices. The ratio of $B^+ : B^0$ decays in the charged (neutral) sample is 1.8 : 1 (1 : 2.3). A maximum likelihood fit procedure finds the following preliminary results:

$$\begin{aligned}
\tau_{B^+} &= 1.69 \pm 0.06\,(\mathrm{stat}) \pm 0.06\,(\mathrm{syst})\ \mathrm{ps},\\
\tau_{B^0} &= 1.63 \pm 0.07\,(\mathrm{stat}) \pm 0.08\,(\mathrm{syst})\ \mathrm{ps},\\
\tau_{B^+}/\tau_{B^0} &= 1.04\ ^{+0.08}_{-0.07}\,(\mathrm{stat}) \pm 0.06\,(\mathrm{syst}).
\end{aligned}$$

Paper Contributed to the XXVIII International Conference on High Energy Physics, July/96, Warsaw, Poland

*This work was supported by Department of Energy contracts: DE-FG02-91ER40676 (BU), DE-FG03-92ER40701 (CIT), DE-FG03-91ER40618 (UCSB), DE-FG03-92ER40689 (UCSC), DE-FG03-93ER40788 (CSU), DE-FG02-91ER40672 (Colorado), DE-FG02-91ER40677 (Illinois), DE-AC03-76SF00098 (LBL), DE-FG02-92ER40715 (Massachusetts), DE-AC02-76ER03069 (MIT), DE-FG06-85ER40224 (Oregon), DE-AC03-76SF00515 (SLAC), DE-FG05-91ER40627 (Tennessee), DE-AC02-76ER00881 (Wisconsin), DE-FG02-92ER40704 (Yale); National Science Foundation grants: PHY-91-13428 (UCSC), PHY-89-21320 (Columbia), PHY-92-04239 (Cincinnati), PHY-88-17930 (Rutgers), PHY-88-19316 (Vanderbilt), PHY-92-03212 (Washington); the UK Science and Engineering Research Council (Brunel and RAL); the Istituto Nazionale di Fisica Nucleare of Italy (Bologna, Ferrara, Frascati, Pisa, Padova, Perugia); and the Japan-US Cooperative Research Project on High Energy Physics (Nagoya, Tohoku).

The spectator model predicts that the lifetime of a heavy hadron depends upon the properties of the constituent weakly decaying quark and is independent of the remaining, or spectator, quarks in the hadron. This model is seen to fail for the charm hadron system for which the lifetime hierarchy $\tau_{D^+} \sim 2\frac{1}{4}\tau_{D_s^+} \sim 2\frac{1}{2}\tau_{D^0} \sim 5\tau_{\Lambda_c^+}$ is observed. QCD corrections to the spectator model are predicted to scale with $1/m_Q^2$ and the B hadron lifetimes are therefore expected to differ by less than 10% [1]. Hence a measurement of the B^+ and B^0 lifetimes and their ratio provide a test of the expected deviations from the spectator model. The analysis is performed on the 1993-5 data sample of 150,000 Z^0 decays collected by the SLAC Large Detector (SLD), at the SLAC Linear Collider (SLC).

The excellent 3D vertexing capabilities of SLD are exploited to identify B hadron vertices produced in hadronic Z^0 decays with high efficiency. This is achieved with a novel topological vertexing technique for reconstructing the secondary vertices produced by weakly decaying hadrons in jets [2]. The decay length is measured using the reconstructed vertex location while the B meson charge is determined from the total charge of the tracks associated with the vertex. This inclusive technique has the advantage of a large efficiency for reconstructing the B vertex since there is no requirement on specific topologies (such as semileptonic B decays).

The components of the SLD[3] utilised by this analysis are the Central Drift Chamber (CDC)[4] for charged track identification and momentum measurement and the CCD pixel Vertex Detector (VXD)[5] for precise position measurements near the interaction point. These systems are immersed in the 0.6 T field of the SLD solenoid. Charged tracks reconstructed in the CDC are linked with pixel clusters in the VXD by extrapolating each track and selecting the best set of associated clusters[4]. A combined fit is performed and the track parameters are recalculated, accounting for multiple scattering. The momentum resolution of the combined fit is $\delta p_T/p_T = \sqrt{(0.01)^2 + (0.0026/p_T)^2}$, where p_T is the track momentum transverse to the beam axis in GeV/c. For a typical track from the primary vertex or heavy hadron decay, the total efficiency of reconstruction in the CDC and linking to a correct set of VXD hits is 94% for the region $|\cos\theta| < 0.74$. The overall track impact parameter resolutions are 11μm and 38μm in the $r\phi$ and rz projections respectively at high momentum, while multiple scattering contributions are $70/p\sin^{3/2}\theta$ μm in both projections.

The micron-sized SLC Interaction Point (IP) centroid position in the xy plane transverse to the beam axis is reconstructed with a measured precision of $\sigma_{IP} = (7 \pm 2)\mu$m using tracks in sets of ~ 30 sequential hadronic Z^0 decays. The median z position of tracks at their point of closest approach to the IP in the xy plane is used to determine the z position of the Z^0 primary vertex on an event-by-event basis. A precision of $\sim 52\mu$m on this quantity is estimated using $Z^0 \to b\bar{b}$ Monte Carlo.

The Monte Carlo events are generated using JETSET 7.4 [6]. The B meson decays are simulated using the CLEO B decay model [7][8] tuned to reproduce the spectra and multiplicities of charmed hadrons, pions, kaons, protons and leptons as measured at the $\Upsilon(4S)$ by ARGUS and CLEO [9]. The branching fractions of the charm hadrons are, in turn, tuned to the existing measurements [10]. The B mesons and baryons are generated with a lifetime of 1.55 ps and 1.10 ps respectively, while the b-quark fragmentation follows the Peterson *et al.* parametrization [13]. The SLD detector is simulated using GEANT 3.21 [11].

Hadronic Z^0 event selection requires at least 7 CDC tracks which pass within 5 cm of the IP in z at the point of closest approach to the beam and which have $P_T >$200 MeV/c. The total energy of the tracks passing these cuts must be greater than 18 GeV. These requirements on the CDC tracking information remove background from $Z^0 \to l^+l^-$ events and two-photon interactions. In addition the thrust axis determined from clusters in the calorimeter must pass $|\cos\theta| < 0.71$, within the acceptance of the vertex detector, and at least three tracks must have two or more linked VXD hits. These selection requirements yield a data sample of 96,000 hadronic Z^0 decays.

Well measured tracks are selected in these events. The CDC track must begin at a radius<39cm, and have $\geq$40 hits to insure that the lever arm provided by the CDC is appreciable. The CDC tracks are also required to extrapolate to within 1cm of the IP in xy, and within 1.5cm in z to eliminate tracks from interaction with the detector material. The fit of the track must satisfy (χ^2/d.o.f.$<$ 5). At least one good VXD link is required, and the combined CDC/VXD fit must also satisfy (χ^2/d.o.f.$<$ 5). The track must have $P_T >$400 MeV/c. The selected tracks are divided into two hemispheres using the event thrust axis which is determined by the SLD calorimetry [4].

The topological vertex reconstruction is applied separately to the tracks in each hemisphere. This analysis is the first application of the algorithm which is described in detail in Ref. [2] and summarized here. The vertices are reconstructed in 3D co-ordinate space by defining a vertex probability $V(\mathbf{r})$ at each position $\mathbf{r}$. The helix parameters for each track i are used to describe the 3D track trajectory as a Gaussian tube $f_i(\mathbf{r})$, where the width of the tube is the uncertainty in the measured track location close to the IP. $V(\mathbf{r})$ is defined as a function of the $f_i(\mathbf{r})$ such that it is sensitive to the track multiplicity at $\mathbf{r}$ and is small in regions where less than two tracks (required for a vertex) have significant $f_i(\mathbf{r})$. A further function $f_0(\mathbf{r})$ is used to describe the location and uncertainty of the IP. This function is combined with the $f_i(\mathbf{r})$ in the definition of $V(\mathbf{r})$ in order to later identify the tracks forming the primary vertex. Maxima are found in $V(\mathbf{r})$ and clustered into spatial regions using a resolution criterion such that two maxima are resolved if the value of $V(\mathbf{r})$ on a straight line between the maxima falls below 60% of the value of $V(\mathbf{r})$ at either maxima. Tracks are associated with these resolved regions to form a set of topological vertices.

The efficiency for reconstructing non-primary vertices is a function of the true decay length of the parent particle. For B hadron decays at $>$ 3mm from the IP this efficiency is about 80%. The efficiency falls at shorter decay length as it becomes harder to resolve the secondary vertex from the primary. The inclusive efficiency for reconstructing at least one secondary vertex in a b hemisphere is $\sim$ 50% (cf. an efficiency of $\sim$ 15% in charm hemispheres and $\sim$ 3% in light quark hemispheres) while the efficiency for finding both a secondary and a tertiary vertex is $\sim$ 5%. For the b hemispheres containing secondary vertices, a 'seed' vertex is chosen to be the non-primary topological vertex furthest from the IP. The seed vertex is rejected if it consists of two oppositely charged tracks with an invariant mass in the range 491–505 MeV/c^2 to remove $K_s^0 \rightarrow \pi^+\pi^-$ decays. If such a rejected seed was a topological tertiary vertex then the two tracks are discarded and the secondary is used as the seed vertex.

A vertex axis is formed by a straight line joining the IP to the seed vertex. The 3D distance of closest approach of a track to the vertex axis, T, and the distance from the IP along the vertex axis to this point, L, are calculated for all tracks. Monte Carlo studies show that tracks which are not associated with the seed vertex but which pass T$<$ 0.1cm and L/D$>$ 0.3 are more likely to be associated with the B decay sequence than to have an alternative origin. Hence such tracks are added to the set of tracks in the seed vertex to form the reconstructed B vertex. This secondary vertex contains tracks from both the B and cascade D decays. The distance from the IP to the vertex determined from all of the tracks now forming the secondary is the reconstructed decay length. Since the purity of the B charge reconstruction is lower for decays close to the IP where tracks are more likely to be wrongly assigned, vertices with decay length $<$ 1mm are discarded.

The mass of the reconstructed vertex is calculated by assuming each track forming the secondary vertex has the mass of a pion. The purity of the charge tag is more likely to be eroded by losing tracks from the B decay chain through track selection inefficiencies and track mis-assignment than by gaining mis-assigned tracks originating from the primary or other background to the B decay. The vertices from which B tracks have been lost tend to have lower mass as well as lower purity. Hence the vertex mass is required to be > 2 GeV/c^2 to select high purity charged and neutral samples. A comparison of the reconstructed mass of the vertex (before the cut) between data and Monte Carlo is shown in Fig. 1. This figure shows that a large fraction of the charm and light flavour contamination in the sample is eliminated by the 2 GeV/c^2 mass cut. Application of this cut yields a sample of 9719 reconstructed B vertices.

To improve the secondary vertex charge reconstruction, tracks which fail the initial selection but have P_T >200 MeV/c and $\sqrt{\sigma_{r\phi}^2 + \sigma_z^2} < 700\mu$m are considered, where $\sigma_{r\phi}$ (σ_z) is the uncertainty in the track position transverse (longitudinal) to the beam direction close to the IP. The charge of these tracks which also pass the cuts T$<$ 0.1cm and L/D$>$ 0.3 is added to the secondary vertex charge.

The charged sample consists of hemispheres with secondary vertex charge, defined above, equal to $\pm$ 1,2 or 3, while the neutral sample consists of the secondary vertices with charge equal to 0. This separates the reconstructed decays into a charged sample of 6033 vertices and a neutral sample of 3665 vertices. Monte Carlo studies indicate that the resulting charged sample is 97.3% pure in B hadrons consisting of 54.6% B^+, 30.5% B^0, 8.6% B_s^0, and 3.6% B baryons. Similarly, the neutral sample is 98.0% pure in B hadrons consisting of 23.3% B^+, 54.5% B^0, 14.6% B_s^0 and 5.6% B baryons. Fig. 2 shows a comparison of the reconstructed charge between data and Monte Carlo.

A further cross check on the charge assignment can be made for the charged B sample, exploiting the large polarized forward-backward asymmetry of b quark production with high electron beam polarization at the SLC. The b quarks are preferencially produced toward the electron (positron) beam direction for the left-handed (right-handed) electron beam. The distribution of the cosine of the event thrust axis polar angle ($\cos\theta_T$), signed by the product of electron beam polarization and reconstructed B vertex charge, is shown in Fig. 3 (separately for 1993 and 1994-95 with average beam polarizations of 63% and 77% respectively). If the vertex charge assignment had unexpected dilution from more mis-assigned B^0's or even the opposite sign $B^\pm$, the observed asymmetry in the signed $\cos\theta_T$ distribution would to be flattened. The good agreement between data and Monte Carlo as shown in Fig. 3 confirms the charge assignment purity predicted by the Monte Carlo.

The lifetimes are extracted from the decay length distributions (over the range 1 mm to 25 mm) of the selected secondary vertices using a binned maximum likelihood technique. The fitting functions are obtained from Monte Carlo decay length distributions for the charged and neutral samples for arbitrary values of the B^+ and B^0 lifetimes (τ^+ and τ^0 respectively), by reweighting the $B^{+,0}$ entries contributing to the Monte Carlo decay length distributions with

$$W^{+,0}(t, \tau^{+,0}) \;=\; \frac{\frac{1}{\tau^{+,0}}\; e^{-t/\tau^{+,0}}}{\frac{1}{\tau_{gen}}\; e^{-t/\tau_{gen}}}, \qquad (1)$$

where τ_{gen} (= 1.55 ps) is the lifetime value used in the Monte Carlo generation and t is the proper time of a given decay. A two parameter fit yields the B^+ and B^0 lifetimes together with the ratio τ_{B^+}/τ_{B^0}. The decay length distributions for the charged and neutral samples are shown in Fig. 4. The bin size used in the fit increases with decay length such that the number of entries per bin is approximately constant. The maximum likelihood fit yields lifetimes of $\tau_{B^+} = 1.69 \pm 0.06$ ps and $\tau_{B^0} = 1.63 \pm 0.07$ ps, with a ratio of $\tau_{B^+}/\tau_{B^0} = 1.04^{+0.08}_{-0.07}$.

We have investigated the systematic uncertainties due to detector and physics modeling, as well as those related to the fitting procedure. Table 1 summarizes the systematic errors on the B^+ and B^0 lifetimes and their ratio. The main detector modeling systematic errors originate from the uncertainties in the track reconstruction efficiency and detector resolution. The observed average charged multiplicity in all hadronic events is $\sim$0.3 tracks fewer in the data compared to the Monte Carlo. A systematic error is derived by assuming this being due to extra tracking inefficiency not simulated by the Monte Carlo. Monte Carlo tracks are randomly removed with dependence on the track momentum and angles to match the data charged track multiplicity and the effect from this entire correction is taken as a systematic error. The Monte Carlo track negative impact parameter distribution (signed by track crossing jet axis in front or behind the IP) agrees very well with the data for both the core and tail in the rϕ view. The signed distribution of track distance to the primary vertex in z (Z_{doca}) at the track $r\phi$ closet approach to the primary vertex, on the other hand, does show some discrepancy between data and Monte Carlo mainly in the core of the distribution while there is good agreement in the negative tail. This is mainly due to remaining vertex detector misalignments. Corrections are applied to the Monte Carlo track Z_{doca} with ϕ dependent systematic shifts up to 20 μm and a random Gaussian smear with $\sigma = 20\mu m/sin\theta$. The total effect of applying this resolution correction is again assigned as a systematic error. We have also made cross checks by performing the lifetime fits for B decay candidates in different ϕ regions and different data taking time periods separately. The results are found to be consistent within statistics.

The physics modeling systematic uncertainties were determined as follows. The b quark fragmentation systematic error was deduced by varying the ϵ_b parameter such that $< x_E >= 0.700 \pm 0.011$ [12] in the Peterson fragmentation function [13]. The shape of the x_E distribution was also varied[14]. The four branching fractions of $\overset{+}{B^0} \rightarrow \overset{+}{D^0}X$ productions were varied by the uncertainty in the current world average [10]. The the fraction of B decays producing two D hadrons was assumed to be 15$\pm$5%. The average B^+ and B^0 decay multiplicities were varied by $\pm$0.3 tracks [16] in an anticorrelated manner. The B_s^0 and B baryon lifetimes and production fractions were varied according to $\tau(B_s^0) = 1.55 \pm 0.15$ ps, $\tau(B \text{ baryon}) = 1.10 \pm 0.11$ ps, $f(B_s^0) = 0.12 \pm 0.04$, and $f(B \text{ baryon}) = 0.08 \pm 0.04$. To account for the uncertainty in the D meson spectrum from B decays an error was assigned by requiring the Monte Carlo spectra to match recent CLEO data [9]. The systematic errors due to uncertainties in charmed meson decay topology were estimated by changing Monte Carlo D decay charged multiplicity and K^0 production according to the uncertainty in experimental measurements [15]. Finally, the lifetime of charm hadrons (D^+, D^0, D_s, Λ_c) was varied according to the uncertainty in their world average [10].

The fitting uncertainties were determined by varying the bin size used in the decay length distributions, and by modifying the cuts on the minimum (no cut–2 mm) and maximum (12–25 mm) decay lengths used in the fit. Fit results are found to be consistent within statistics for these variations, but a systematic error is conservatively assigned using the RMS variation of the results.

In summary, from 150,000 Z^0 decays collected by SLD between 1993 and 1995 the B^+ and B^0 lifetimes have been measured using a novel topological vertexing technique. The analysis isolates 9698 B hadron candidates, with a sample purity estimated to be $> 97\%$, and determines the following preliminary values for the lifetimes of the B^+ and B^0 mesons:

$$\langle \tau_{B^+} \rangle = 1.69 \pm 0.06(\mathrm{stat}) \pm 0.06(\mathrm{syst})\mathrm{ps} \tag{2}$$

$$\langle \tau_{B^0} \rangle = 1.63 \pm 0.07(\mathrm{stat}) \pm 0.08(\mathrm{syst})\mathrm{ps} \tag{3}$$

$$\frac{\langle \tau_{B^+} \rangle}{\langle \tau_{B^0} \rangle} = 1.04^{+0.08}_{-0.07}(\mathrm{stat}) \pm 0.06(\mathrm{syst}) \tag{4}$$

We thank the personnel of the SLAC accelerator department and the technical staffs of our collaborating institutions for their outstanding efforts.

References

[1] I.I. Bigi *et al.*, *Non-leptonic Decays of Beauty Hadrons - from Phenomenology to Theory,* in *B Decays*, ed. S. Stone, World Scientific (1994).

[2] D. J. Jackson, **SLAC-PUB-7215** (1996), submitted to *Nucl. Inst. and Meth.*, *A Topological Vertex Reconstruction Algorithm for Hadronic Jets.*

[3] G. Agnew *et al.*, *SLD Design Report*, SLAC-Report-273 (1984).

[4] K. Abe *et al.*, Phys. Rev. **D53**, 1023 (1996).

[5] G.D. Agnew *et al.*, "Design and Performance of the SLD Vertex Detector, a 120 MPixel Tracking System", Proceedings of the XXVI International Conference on High Energy Physics, Dallas, Texas, 6–12 August, 1992,
M. Strauss *et al.*, "Performance of the SLD CCD Pixel Vertex Detector and Design of an Upgrade," Proceedings of the 27th International Conference on High Energy Physics, Glasgow, Scotland, July 20-27, 1994.

[6] T. Sjöstrand, CERN-TH-7112-93, Feb. 1994.

[7] CLEO QQ MC code provided by P. Kim and the CLEO Collaboration.

[8] T. R. Junk, Ph.D. Thesis, Stanford University, SLAC-Report-95-476, Nov. 1995.

[9] CLEO Collaboration: B. Barish *et al.*, **CLNS-95-1362** (1995);
ARGUS Collaboration: H. Albrecht *et al.*, *Z. Phys.* **C58**, 191 (1993);
ARGUS Collaboration: H. Albrecht *et al.*, *Z. Phys.* **C62**, 371 (1994);
F. Muheim (CLEO Collaboration), talk presented at the 8th DPF Meeting, Albuquerque, New Mexico, Aug 1994;

M. Thulasidas, Ph.D thesis, Syracuse University (1993);
CLEO Collaboration: G. Crawford *et al.*, *Phys. Rev.* **D45**, 752 (1992)
CLEO Collaboration: D. Bortoletto *et al.*, *Phys. Rev.* **D45**, 21 (1992).

[10] Particle Data Group, Phys. Rev. **D50**, Part I (1994).

[11] R. Brun *et al.*, CERN-DD/EE/84-1, 1989.

[12] see for example, R. Akers *et al.*, Z. Phys. **C60**, 601 (1993); D. Buskulic *et al.*, Z. Phys. **C62**, 1 (1994); D. Buskulic *et al.*, Z. Phys. **C62**, 179 (1994); P. Abreu *et al.*, Z. Phys. **C66**, 323 (1995).

[13] C. Peterson *et al.*, Phys. Rev. **D27**, 105 (1983).

[14] M. G. Bowler, Z. Phys. **C11**, 169 (1981).

[15] D.Coffman *et al.*, Phys. Lett. **B263**, 135 (1991).

[16] H.Albrecht *et al.*, Z. Phys. **C54**, 13 (1992); R.Giles *et al.*, Phys. Rev. **D30**, 2279 (1984).

**List of Authors

K. Abe,(19) K. Abe,(29) I. Abt,(13) T. Akagi,(27) N.J. Allen,(4) W.W. Ash,(27)†
D. Aston,(27) K.G. Baird,(24) C. Baltay,(33) H.R. Band,(32) M.B. Barakat,(33)
G. Baranko,(9) O. Bardon,(15) T. Barklow,(27) A.O. Bazarko,(10) R. Ben-David,(33)
A.C. Benvenuti,(2) G.M. Bilei,(22) D. Bisello,(21) G. Blaylock,(6) J.R. Bogart,(27)
B. Bolen,(17) T. Bolton,(10) G.R. Bower,(27) J.E. Brau,(20) M. Breidenbach,(27)
W.M. Bugg,(28) D. Burke,(27) T.H. Burnett,(31) P.N. Burrows,(15) W. Busza,(15)
A. Calcaterra,(12) D.O. Caldwell,(5) D. Calloway,(27) B. Camanzi,(11)
M. Carpinelli,(23) R. Cassell,(27) R. Castaldi,(23)(a) A. Castro,(21)
M. Cavalli-Sforza,(6) A. Chou,(27) E. Church,(31) H.O. Cohn,(28) J.A. Coller,(3)
V. Cook,(31) R. Cotton,(4) R.F. Cowan,(15) D.G. Coyne,(6) G. Crawford,(27)
A. D'Oliveira,(7) C.J.S. Damerell,(25) M. Daoudi,(27) R. De Sangro,(12)
R. Dell'Orso,(23) P.J. Dervan,(4) M. Dima,(8) D.N. Dong,(15) P.Y.C. Du,(28)
R. Dubois,(27) B.I. Eisenstein,(13) R. Elia,(27) E. Etzion,(4) D. Falciai,(22) C. Fan,(9)
M.J. Fero,(15) R. Frey,(20) K. Furuno,(20) T. Gillman,(25) G. Gladding,(13)
S. Gonzalez,(15) G.D. Hallewell,(27) E.L. Hart,(28) J.L. Harton,(8) A. Hasan,(4)
Y. Hasegawa,(29) K. Hasuko,(29) S. J. Hedges,(3) S.S. Hertzbach,(16)
M.D. Hildreth,(27) J. Huber,(20) M.E. Huffer,(27) E.W. Hughes,(27) H. Hwang,(20)
Y. Iwasaki,(29) D.J. Jackson,(25) P. Jacques,(24) J. A. Jaros,(27) A.S. Johnson,(3)
J.R. Johnson,(32) R.A. Johnson,(7) T. Junk,(27) R. Kajikawa,(19) M. Kalelkar,(24)
H. J. Kang,(26) I. Karliner,(13) H. Kawahara,(27) H.W. Kendall,(15) Y. D. Kim,(26)
M.E. King,(27) R. King,(27) R.R. Kofler,(16) N.M. Krishna,(9) R.S. Kroeger,(17)
J.F. Labs,(27) M. Langston,(20) A. Lath,(15) J.A. Lauber,(9) D.W.G.S. Leith,(27)

V. Lia,[15] M.X. Liu,[33] X. Liu,[6] M. Loreti,[21] A. Lu,[5] H.L. Lynch,[27] J. Ma,[31] G. Mancinelli,[22] S. Manly,[33] G. Mantovani,[22] T.W. Markiewicz,[27] T. Maruyama,[27] H. Masuda,[27] E. Mazzucato,[11] A.K. McKemey,[4] B.T. Meadows,[7] R. Messner,[27] P.M. Mockett,[31] K.C. Moffeit,[27] T.B. Moore,[33] D. Muller,[27] T. Nagamine,[27] S. Narita,[29] U. Nauenberg,[9] H. Neal,[27] M. Nussbaum,[7] Y. Ohnishi,[19] L.S. Osborne,[15] R.S. Panvini,[30] H. Park,[20] T.J. Pavel,[27] I. Peruzzi,[12][b] M. Piccolo,[12] L. Piemontese,[11] E. Pieroni,[23] K.T. Pitts,[20] R.J. Plano,[24] R. Prepost,[32] C.Y. Prescott,[27] G.D. Punkar,[27] J. Quigley,[15] B.N. Ratcliff,[27] T.W. Reeves,[30] J. Reidy,[17] P.E. Rensing,[27] L.S. Rochester,[27] P.C. Rowson,[10] J.J. Russell,[27] O.H. Saxton,[27] T. Schalk,[6] R.H. Schindler,[27] B.A. Schumm,[14] S. Sen,[33] V.V. Serbo,[32] M.H. Shaevitz,[10] J.T. Shank,[3] G. Shapiro,[14] D.J. Sherden,[27] K.D. Shmakov,[28] C. Simopoulos,[27] N.B. Sinev,[20] S.R. Smith,[27] M.B. Smy,[8] J.A. Snyder,[33] P. Stamer,[24] H. Steiner,[14] R. Steiner,[1] M.G. Strauss,[16] D. Su,[27] F. Suekane,[29] A. Sugiyama,[19] S. Suzuki,[19] M. Swartz,[27] A. Szumilo,[31] T. Takahashi,[27] F.E. Taylor,[15] E. Torrence,[15] A.I. Trandafir,[16] J.D. Turk,[33] T. Usher,[27] J. Va'vra,[27] C. Vannini,[23] E. Vella,[27] J.P. Venuti,[30] R. Verdier,[15] P.G. Verdini,[23] S.R. Wagner,[27] A.P. Waite,[27] S.J. Watts,[4] A.W. Weidemann,[28] E.R. Weiss,[31] J.S. Whitaker,[3] S.L. White,[28] F.J. Wickens,[25] D.A. Williams,[6] D.C. Williams,[15] S.H. Williams,[27] S. Willocq,[33] R.J. Wilson,[8] W.J. Wisniewski,[27] M. Woods,[27] G.B. Word,[24] J. Wyss,[21] R.K. Yamamoto,[15] J.M. Yamartino,[15] X. Yang,[20] S.J. Yellin,[5] C.C. Young,[27] H. Yuta,[29] G. Zapalac,[32] R.W. Zdarko,[27] C. Zeitlin,[20] and J. Zhou,[20]

[1]*Adelphi University, Garden City, New York 11530*
[2]*INFN Sezione di Bologna, I-40126 Bologna, Italy*
[3]*Boston University, Boston, Massachusetts 02215*
[4]*Brunel University, Uxbridge, Middlesex UB8 3PH, United Kingdom*
[5]*University of California at Santa Barbara, Santa Barbara, California 93106*
[6]*University of California at Santa Cruz, Santa Cruz, California 95064*
[7]*University of Cincinnati, Cincinnati, Ohio 45221*
[8]*Colorado State University, Fort Collins, Colorado 80523*
[9]*University of Colorado, Boulder, Colorado 80309*
[10]*Columbia University, New York, New York 10027*
[11]*INFN Sezione di Ferrara and Università di Ferrara, I-44100 Ferrara, Italy*
[12]*INFN Lab. Nazionali di Frascati, I-00044 Frascati, Italy*
[13]*University of Illinois, Urbana, Illinois 61801*
[14]*Lawrence Berkeley Laboratory, University of California, Berkeley, California 94720*
[15]*Massachusetts Institute of Technology, Cambridge, Massachusetts 02139*
[16]*University of Massachusetts, Amherst, Massachusetts 01003*
[17]*University of Mississippi, University, Mississippi 38677*

[19] *Nagoya University, Chikusa-ku, Nagoya 464 Japan*
[20] *University of Oregon, Eugene, Oregon 97403*
[21] *INFN Sezione di Padova and Università di Padova, I-35100 Padova, Italy*
[22] *INFN Sezione di Perugia and Università di Perugia, I-06100 Perugia, Italy*
[23] *INFN Sezione di Pisa and Università di Pisa, I-56100 Pisa, Italy*
[24] *Rutgers University, Piscataway, New Jersey 08855*
[25] *Rutherford Appleton Laboratory, Chilton, Didcot, Oxon OX11 0QX United Kingdom*
[26] *Sogang University, Seoul, Korea*
[27] *Stanford Linear Accelerator Center, Stanford University, Stanford, California 94309*
[28] *University of Tennessee, Knoxville, Tennessee 37996*
[29] *Tohoku University, Sendai 980 Japan*
[30] *Vanderbilt University, Nashville, Tennessee 37235*
[31] *University of Washington, Seattle, Washington 98195*
[32] *University of Wisconsin, Madison, Wisconsin 53706*
[33] *Yale University, New Haven, Connecticut 06511*
† *Deceased*
[a] *Also at the Università di Genova*
[b] *Also at the Università di Perugia*

Systematic Error	$\Delta\tau_{B^+}$ /ps	$\Delta\tau_{B^0}$ /ps	$\Delta\left(\frac{\tau_{B^+}}{\tau_{B^0}}\right)$
Detector Modeling			
Tracking efficiency	0.005	0.032	0.022
Tracking resolution	0.030	0.003	0.021
Physics Modeling			
b fragmentation	0.036	0.038	0.011
B decay charm	0.012	0.008	0.009
B decay multipl.	0.016	0.008	0.006
B_s^0 fraction	0.012	0.004	0.005
B baryon fraction	0.013	0.041	0.017
B_s^0 lifetime	0.001	0.036	0.022
B baryon lifetime	$<.001$	0.008	0.005
$B \to D$ spectrum	0.006	0.025	0.019
D decay multiplicity	0.011	0.010	0.013
D decay K^0 yield	0.001	0.019	0.012
Charm hadron lifetime	0.002	0.004	0.002
Fit systematics	0.024	0.013	0.022
MC statistics	0.017	0.018	0.021
TOTAL SYSTEMATIC	0.063	0.085	0.060

Table 1: Summary of contributions to the systematic error for the B^+ and B^0 lifetimes and the lifetime ratio.

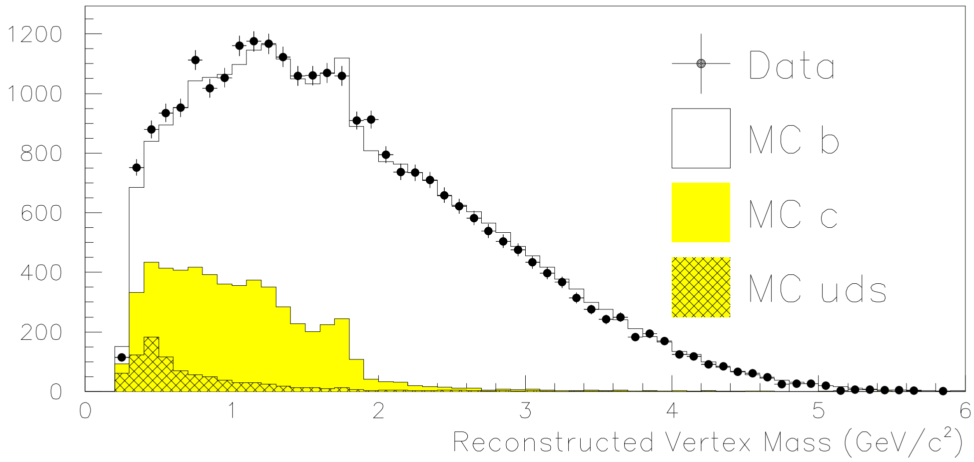

Figure 1: Mass of reconstructed vertex for Monte Carlo (histogram) and data (points).

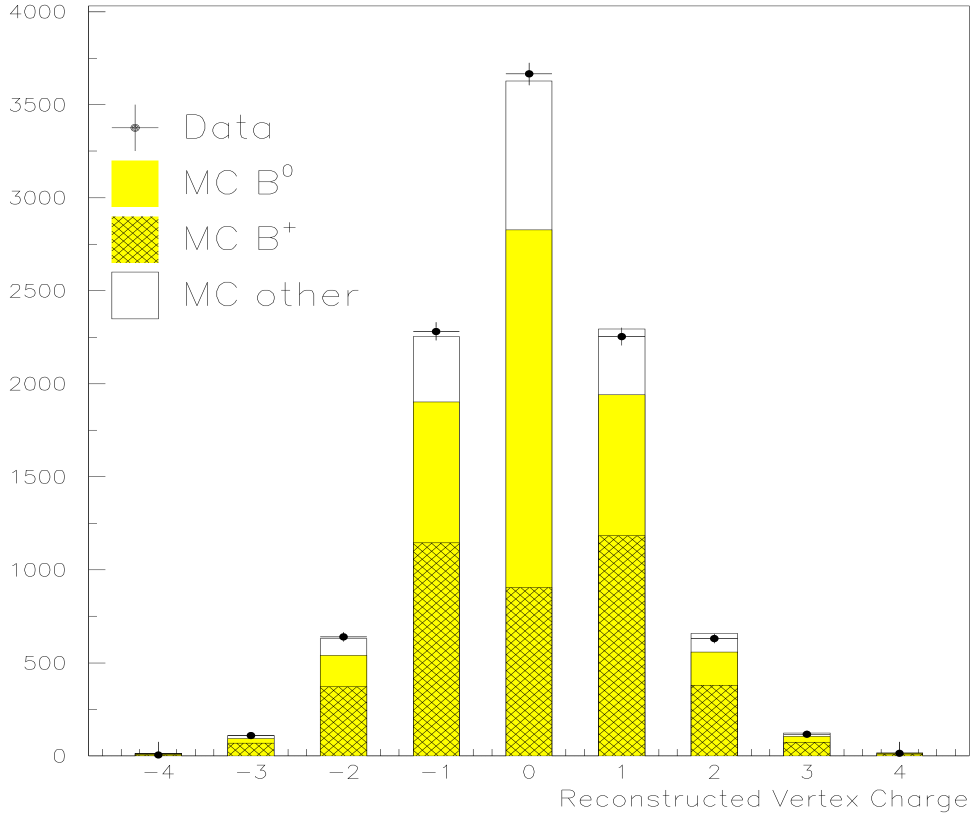

Figure 2: Reconstructed vertex charge for Monte Carlo (histogram) and data (points).

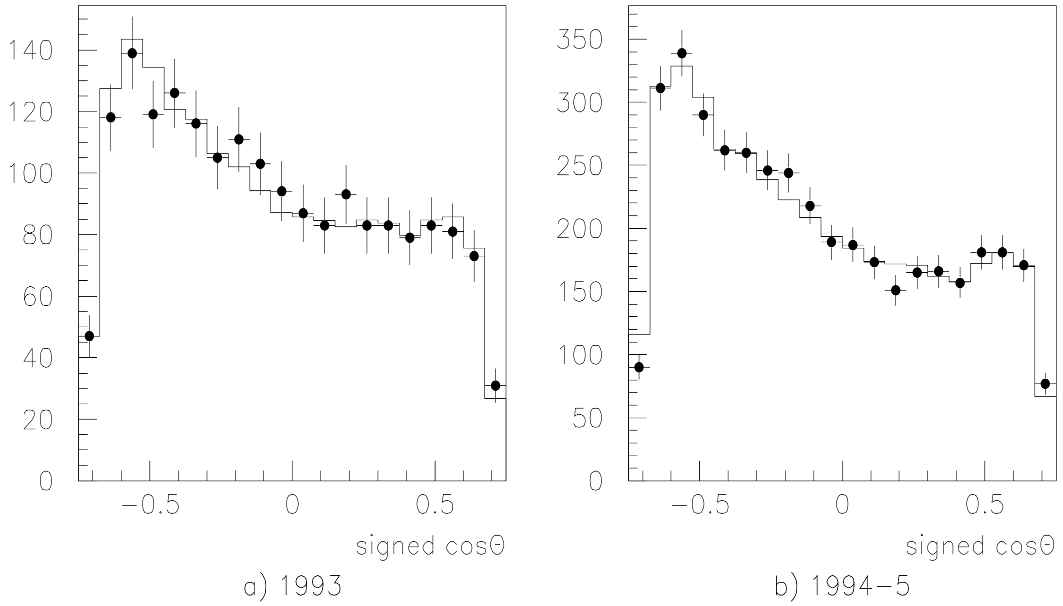

Figure 3: Distributions of B vertex hemisphere event thrust axis with respect to the positron beam, signed by the product of electron polarization and reconstructed charge of the charged B candidates, for data (points) and Monte Carlo (histogram).

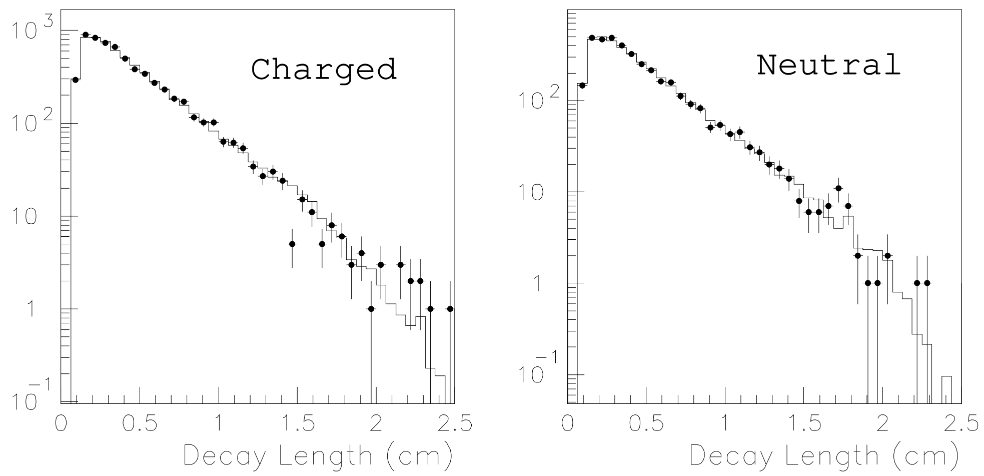

Figure 4: Decay length distributions for best fit Monte Carlo (histogram) and data (points).